Trajectory Analysis of Single Molecules Exhibiting non-Brownian Motion.

Supplemental Information.

Lindsay C.C. Elliott[1], Moussa Barhoum[2], Joel M. Harris[2] and Paul W. Bohn[3]*

[1]Department of Chemistry, University of Illinois at Urbana-Champaign, 600 S. Mathews Ave.,
Urbana, IL   61801

[2]Department of Chemistry, University of Utah, 315 South 1400 East, Salt Lake City, UT 84112

[3]Department of Chemical and Biomolecular Engineering and Department of Chemistry and
Biochemistry, University of Notre Dame, Notre Dame, IN 46556
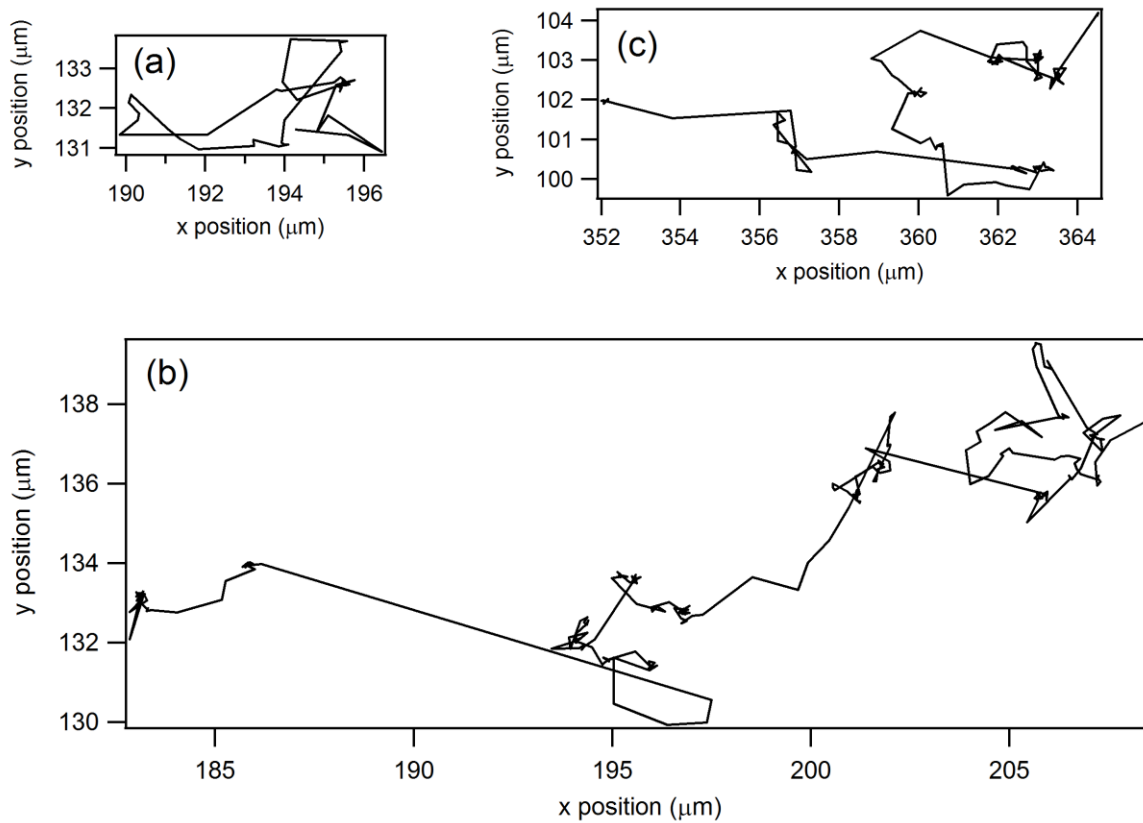
Additional SMT Trajectories

Figure S1: Single molecule trajectories for Molecules 1 (a), 2 (b), and 5 (c), respectively.

Plots are scaled to match *x*- and *y*-axis displacement magnitudes for each trajectory.

Additional Confinement Level Results

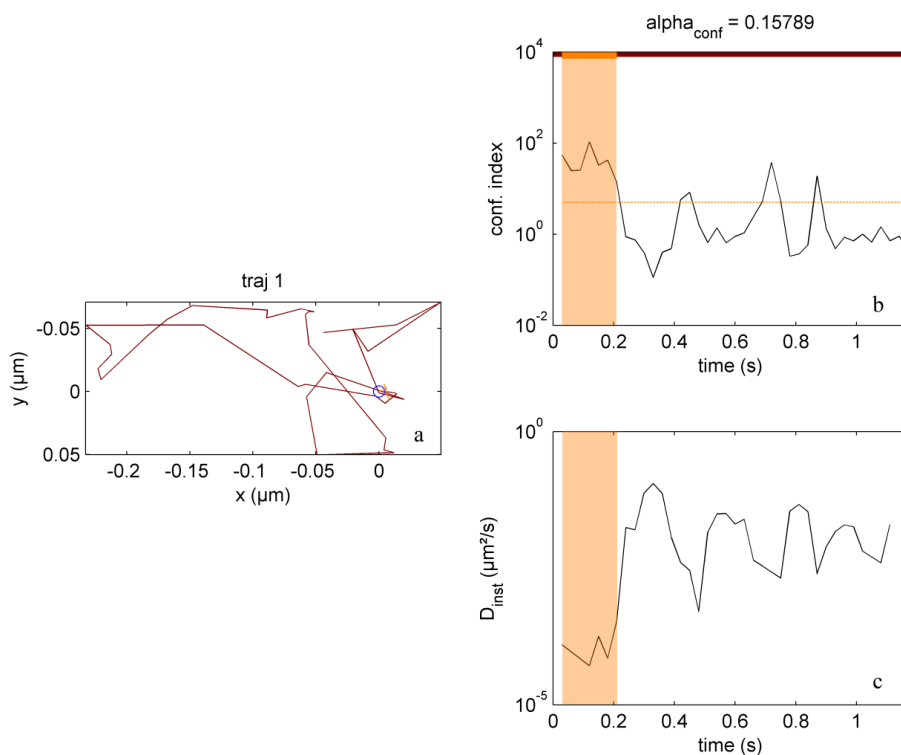The confinement level results for Molecules 1, 2, 3, and 5 are shown in Figures S2-S5.

Figure S2: Confinement level results for Molecule 1. In panel **a** the trajectory is shown with 'free' periods in red and 'confined' periods in orange, the start marked by a blue circle. Panel **b** shows the confinement level L throughout the trajectory. 'Confined' periods are shaded orange and the fraction of confinement α_{conf} is listed above the plot. The minimum confinement level L_{min} is displayed as the horizontal orange line across the plot. Panel **c** shows the instantaneous diffusion coefficient throughout the trajectory. Note the log-scale ordinate in **b** and **c**.
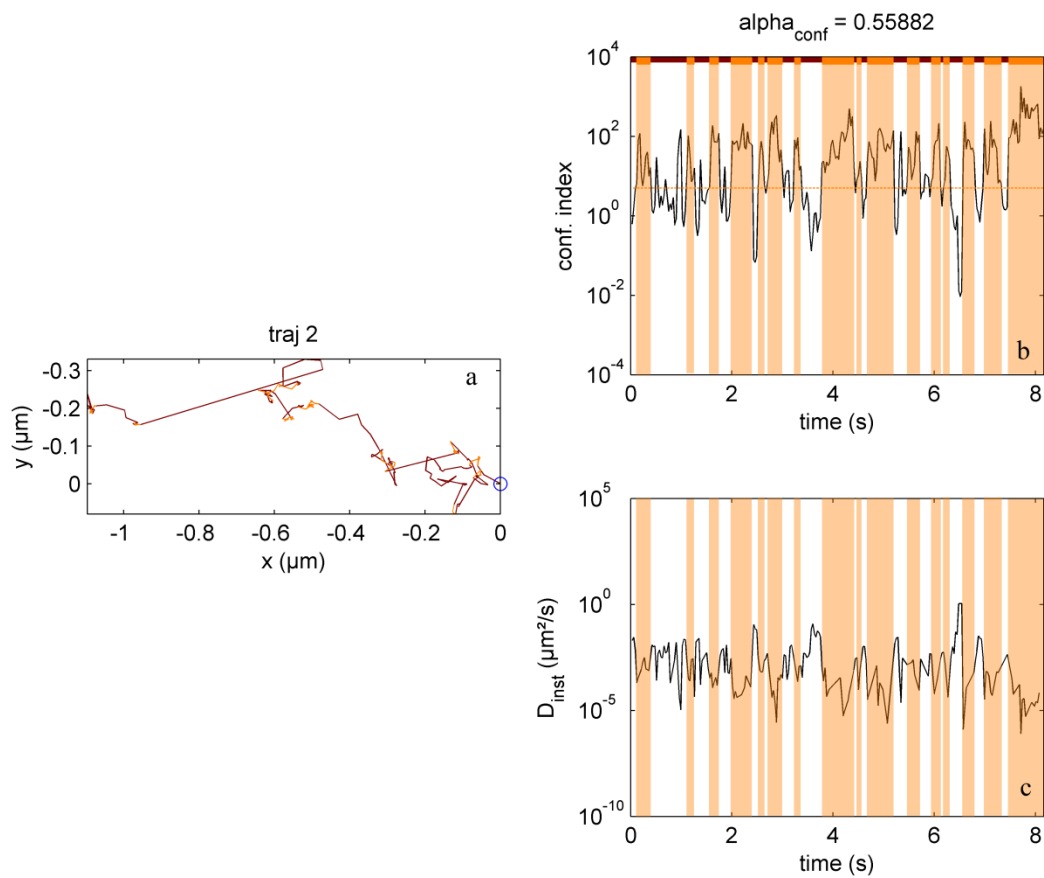
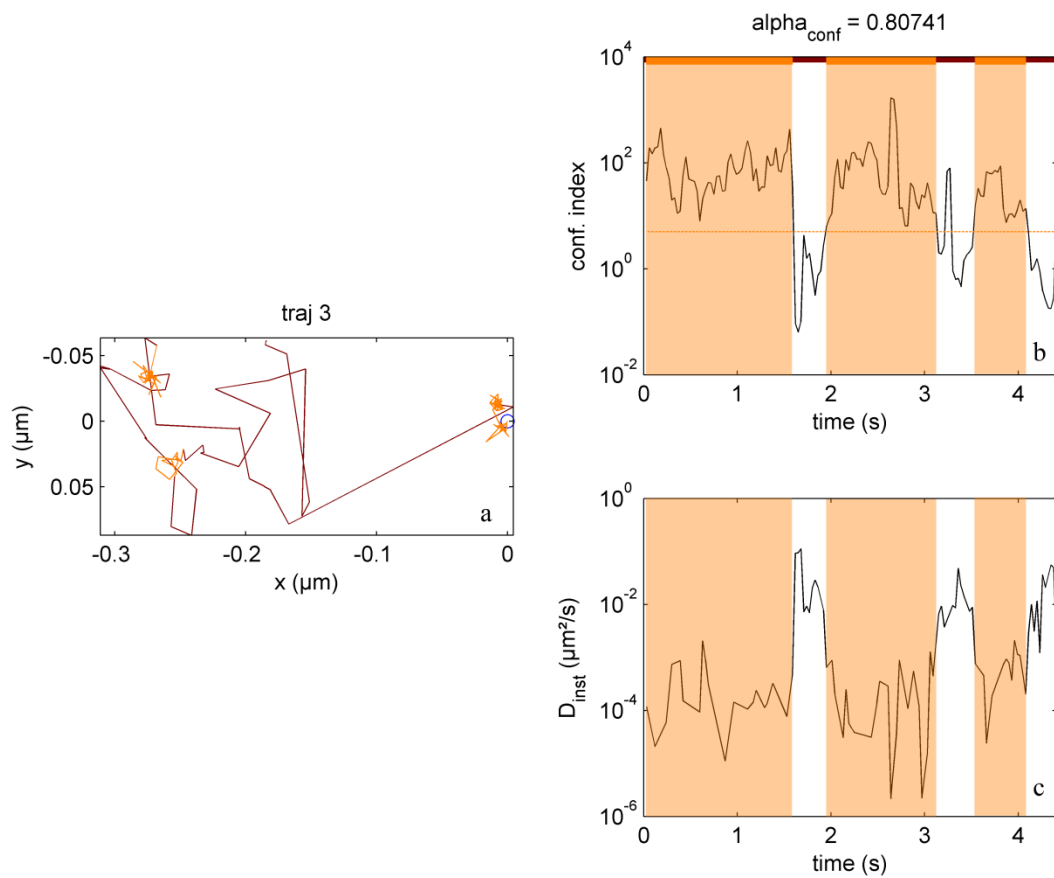Figure S3: Confinement level results for Molecule 2. Plot details as in Fig. S2.

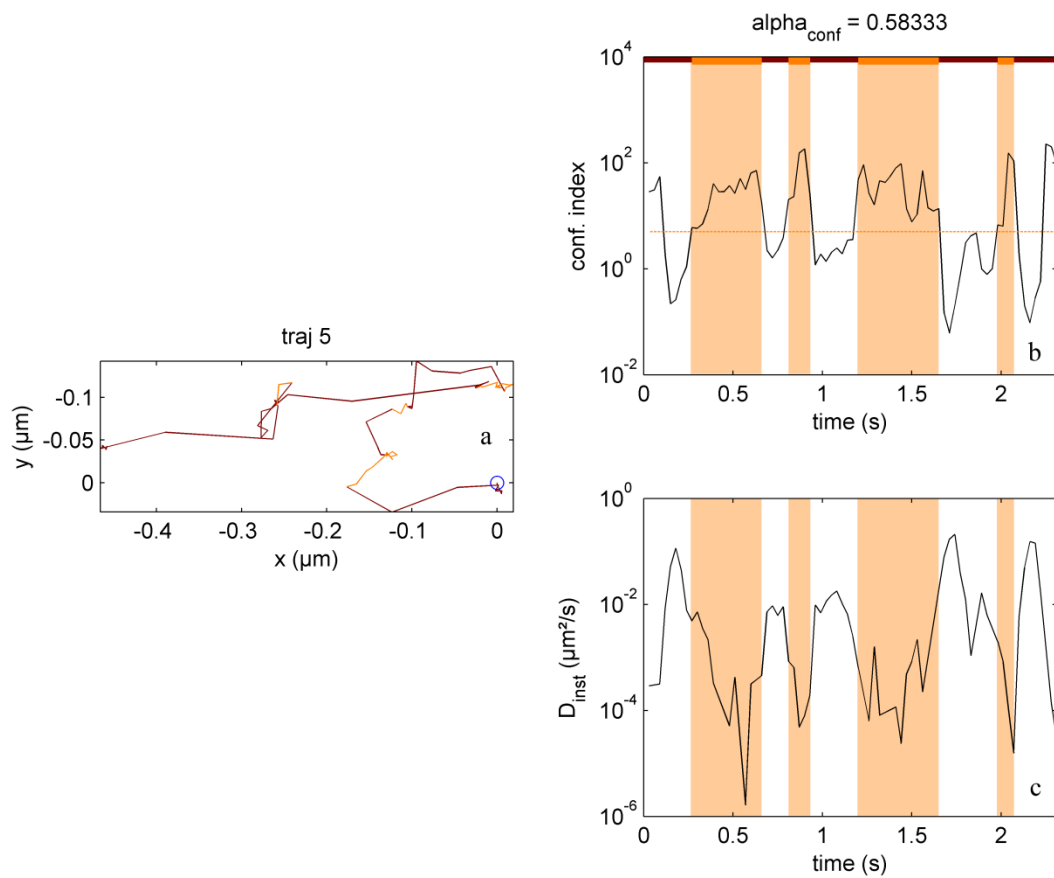Figure S4: Confinement level results for Molecule 3. Plot details as in Fig. S2.

Figure S5: Confinement level results for Molecule 5. Plot details as in Fig. S2.

Additional Time Series Analysis Results

Figures and output tables from Times series analysis. Descriptions of all the values and equations for the models can be found in the original paper and the Matlab software written by the authors, available online[1].

Figure S6: Time series analysis results for Molecule 1. Panel (a) shows MSD data and fitting with two linear and two power law models, panel (b) shows step size distribution data and fitting with general Weibull and Chi models.

Figure S7: Time series analysis results for Molecule 2. Plot details as in Fig. S6.

Figure S8: Time series analysis results for Molecule 3. Plot details as in Fig. S6.

Figure S9: Time series analysis results for Molecule 5. Plot details as in Fig. S6.

Table S1 shows the fitting parameters and least squares residuals found for the mean squared displacement vs. time delay for the linear with offset and power law with offset for all molecules.
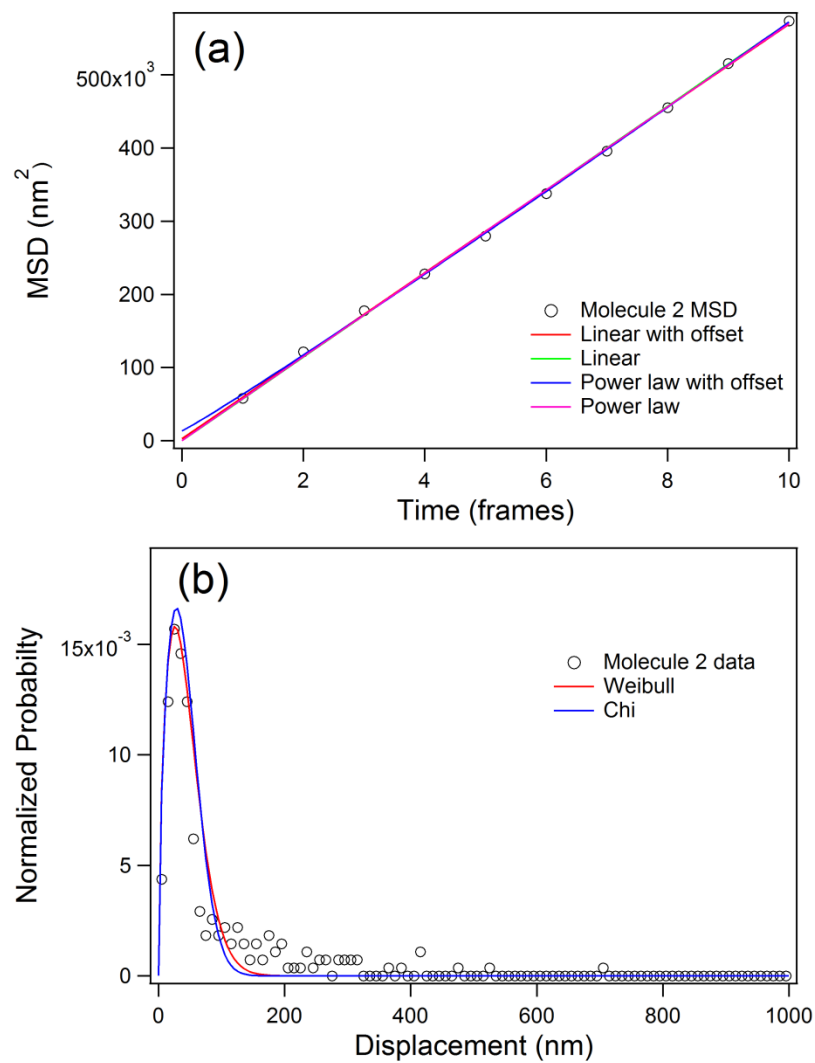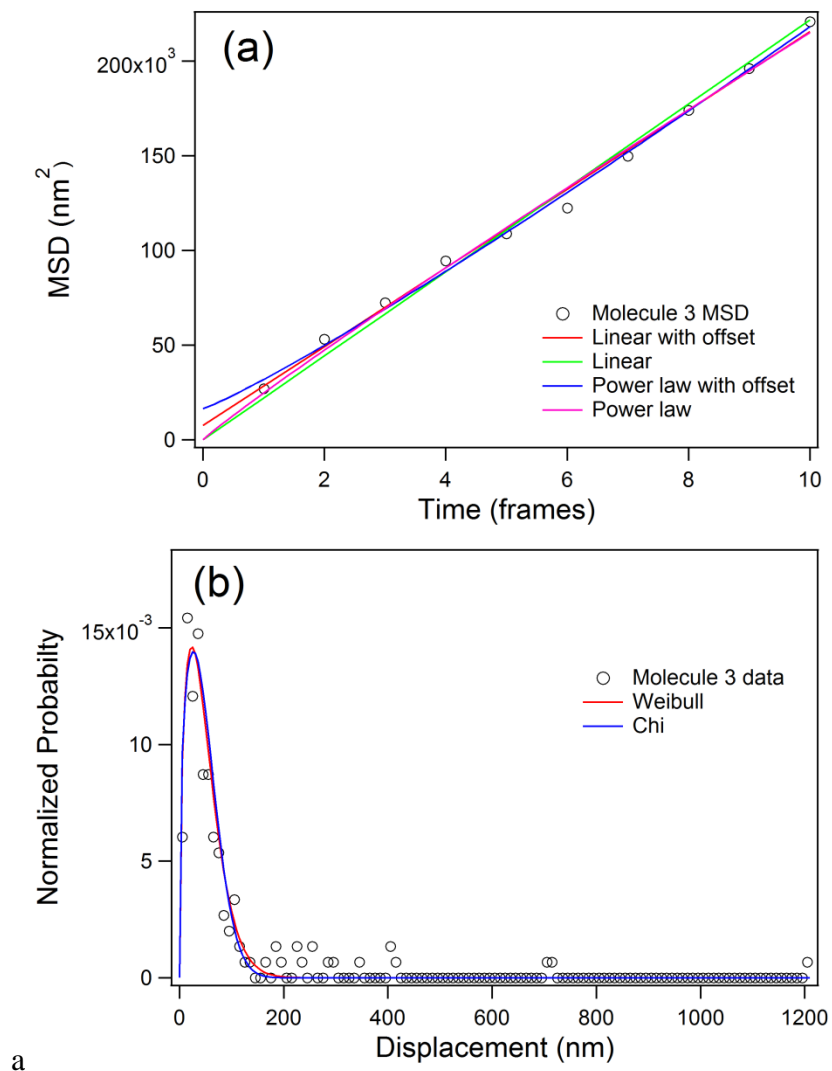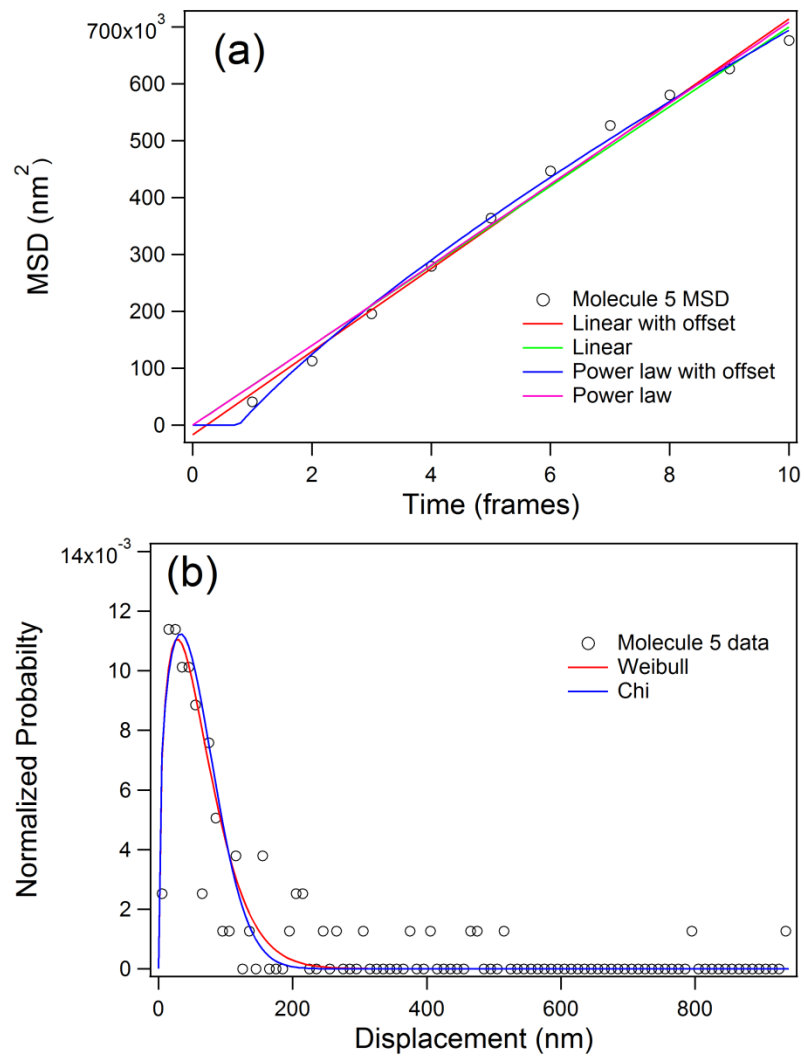
Table S1: Estimates output from time series analysis for all molecules.

Molecule	$A1^a$	B1	R1	$a1^b$	b1	$\alpha 1$	r1
1	97638	-59733	13804	65310	-0.0537	1.1535	46064
2	56646	2893	4035	50244	13196	1.0464	11075
3	20794	7574	4272	24662	-0.0278	0.9404	15308
4	41121	28483	5511	59675	-0.0678	0.8616	15664
5	73111	-17146	20758	144536	-118577	0.7499	43553

[a]$A1$, $B1$, and $R1$ are the optimized parameters and residual, respectively, from the least square fitting for the linear equation with offset: $y = A1*x + B1$

[b]a1, b1, $\alpha 1$ and $r1$ are the optimized parameters and residual, respectively, from the least square fitting for the power law equation with offset: $y = a1*x^{\alpha 1} + b1$

Additional Statistical Analysis and Multistate Kinetics Results

The fitting parameters for the step size distribution fitting from the statistical analysis and multistate kinetics are shown in Table S2.

Table S2: Parameters determined from the step size distribution fitting.

	1 state	2 states	3 states	4 states
D_1	0.4174	0.0239	0.0177	0.0141
D_2	---	1.7412	10.0799	17.6058
D_3	---	---	0.4159	0.1304
D_4	---	---	---	0.9355
x_1	1	0.7709	0.690	0.600
x_2	---	0.2291	0.029	0.014
x_3	---	---	0.282	0.251
x_4	---	---	---	0.135

States 1-4 include the diffusion coefficient(s) first and then the fraction of each population for the step size pdf fits in Figure 7. The most likely number of states is then determined by applying the Akaike information criterion and the diffusion coefficient(s), and the fraction of states for each sub-population is taken from these values for the ensemble of all molecules.

Confinement Level Calculations Applied to Simulated Data

The confinement level calculation algorithm was tested with simulated intermittent slow/fast trajectories. These trials show that when $D_{fast}/D_{slow} = 10$, detection of confinement fairly accurate, even when the fast diffusion is only for 5 frames. On the other hand, when $D_{fast}/D_{slow} < 10$ the reliability of the confinement detection drops sharply.

Table S4: Confinement level results D_{conf}, D_{free}, and α.

Simulation	D_{slow}	D_{fast}	t_{slow}/t_{total}	D_{conf}	D_{free}	α (mean $\pm$ std)
25_25_x100	0.01	1	0.5	0.03	1.5	0.55 $\pm$ 0.07
25_25_x10	0.1	1	0.5	0.13	1.4	0.42 $\pm$ 0.07
25_25_x5	0.2	1	0.5	0.2	1.2	0.28 $\pm$ 0.11
20_5_x10	0.1	1	0.8	0.15	0.62	0.63 $\pm$ 0.08

All calculations were carried out with $D_{global} = 1000*timelag$. Diffusion coefficients, *D*, are in units of $\mu m^2/sec$.

Trajectory analysis was carried out with $[L_c, t_c, S_m] = [5, 3, 4]$. Intermittent motion was simulated in a modified Matlab program[2] (see Experimental section for details). All movies have 100 trajectories in 100 frames, 30 ms exposures, 100X magnification and 0.05 Gaussian noise. Simulation datasets 1-3 were used to test the limits of the analysis techniques in identifying periods of fast and slow diffusion when the difference between diffusion coefficients

is decreased and to test the limits of estimating small diffusion coefficients. Datasets #2 and #4 were used to test the accuracy of the analysis techniques when the period of fast diffusion is very short (only 5 frames). The x_y notation denotes alternating x frames of slow diffusion, then y frames of fast diffusion.

Experimental

Materials. Unless otherwise noted reagents and solvents were obtained from Aldrich. 1,1'-dioctadecyl-3,3,3'3'-tetramethylindocarbocyanine (DiIC$_{18}$, Invitrogen), Rhodamine 6G (99%, Acros), 11-trichlorosilylundecyl-2′-bromo-2-isobutyrate (silane initiator) (95+%, ATRP Solutions), hexanes (ACS reagent, 99.9%, Fisher), dichloromethane (DCM, Chromasol Plus), ethanol (EtOH, denatured for HPLC, Acros), isopropanol (IPA, ACS reagent, >99.5%), cuprous bromide (CuBr, 99.999%), ethanol (EtOH, 99%, Fisher), toluene (ACS spectrophotometric, Sigma Aldrich), acetone (Lab reagent, $\geq$ 99.5%, Sigma Aldrich), hydrogen peroxide (H$_2$O$_2$, 30%, Certified ACS, Fisher Chemical), and sulfuric acid (H$_2$SO$_4$, 95-98%, c.p., Acros Chemicals) were used as received. N-isopropylacrylamide (NIPAAm, 97%) was purified by running a 1:1 hexanes/DCM saturated solution through a 2.5 cm basic alumina column, removing the solvent by reduced pressure evaporation, recrystallizing the remaining solid in hot hexanes at $<$ 50°C, rinsing with minimal ice cold hexanes, and removing the solvent by reduced pressure evaporation. Methanol (MeOH, ACS reagent, 99.9%, Fisher), pentamethyldiethylenetriamine (PMDETA, 99%), deionized(DI) water(ρ = 18 MΩ cm, Millipore Corp.) in Schlenk flasks and toluene (anhydrous, 99.8%, Sigma Aldrich) and triethylamine (TEA, $\geq$ 99.5%, Sigma Aldrich)in SureSeal bottles were degassed by bubbling nitrogen for 5-10 minutes and then were immediately transferred into a controlled atmosphere box.

13

Sample preparation. pNIPAAm brushes 30-100 nm thick dry, ~60-200 nm thick hydrated were prepared by a method described previously.[3, 4] Borosilicate glass coverslips (No. 1.5, Gold Seal, Electron Microscopy Sciences) were prepared by rinsing with DI water and then IPA, drying with a nitrogen stream, and either (1) exposing to argon plasma for 10 min, to strip away the outer layer and any surface contamination, or (2) cleaning any organic contamination in a 1:3 H_2O_2/H_2SO_4 piranha solution. A silane monolayer for ATRP initiation was deposited onto a coverslip in a nitrogen glovebox to control the amount of water in the reaction solution. Following published procedures,[5] the coverslips were immersed in a silanization solution that consisted of 20 mL anhydrous toluene, 150 μL TEA, and 30 μL silane for 15 min. After the reaction period was completed, the coverslips were removed from the controlled atmosphere box, sonicated in fresh non-anhydrous toluene for 5 min, rinsed with acetone and methanol, and dried with a nitrogen stream. A silicon wafer sample was used to check the silane layer thickness for consistency across the sample with ellipsometry and to confirm that 15 minutes was sufficient reaction time. After silanizing each coverslip, the initiated sample was transferred back into the nitrogen controlled atmosphere box for polymerization.

Atom transfer radical polymerization (ATRP) was subsequently carried out by immersing the initiated sample in the reaction solution at 298K in an oxygen-free atmosphere for the desired amount of time. Surface initiated ATRP is a living polymerization that results in relatively homogeneous chain length, low background solution polymerization, controllable film thickness, and minimal crosslinking between chains.[6] The reaction mixture consisted of NIPAAm (3.15 g, 27.5 mmol), CuBr (40.0 mg, 0.278 mmol) and PMDETA (175 μL, 0.835mmol) in 30 mL of 1:1 v:v MeOH:water. When mixing the reactants, a small amount of MeOH and then the PMDETA were added to the CuBr. In a separate container, the remaining MeOH and then the water were

added to the NIPAAm. After all solids dissolved, the two mixtures were added to each other, resulting in a pale green solution, into which the initiated samples were then placed. After the desired amount of time, the samples were removed from the reaction mixture, transferred out of the controlled atmosphere box, rinsed with methanol, and dried with a nitrogen stream. During preliminary experiments atomic force microscopy (Asylum Research MFP-3D), x-ray photoelectron spectroscopy (Kratos Axis ULTRA), single wavelength ellipsometry (Gaertner L116C), and infrared spectroscopy (Nicolet Nexus 670 FT) were used to verify the formation of the initiator and the polymer layers (data not shown). In subsequent preparations, thickness was checked with profilometry (Sloan Dektak[3] ST) and/or ellipsometry.

Single molecule fluorescence microscopy. The microscope is an objective-based total internal reflection fluorescence (TIRF) instrument built on an Olympus IX71 body as illustrated in Figure S10. The excitation source is a 532nm solid-state laser (B&W Tek Inc.) with 25 mW going into the objective. The laser beam is circularly polarized by a quarter-waveplate and coupled into a single-mode, polarization-maintaining fiber optic (Thorlabs). The laser beam is then focused onto the back focal plane of the TIRF objective. The end of the fiber optic and the collimating lens are translated laterally in order to bring the system into total internal reflection. Illumination and collection are both carried out with a 60X 1.45 NA oil immersion objective (Olympus). Images are formed on a back illuminated Cascade II 512 EMCCD (Photometrics). The microscope has a 100-200 nm depth of excitation and an effective pixel size of 267 nm with 60X magnification.
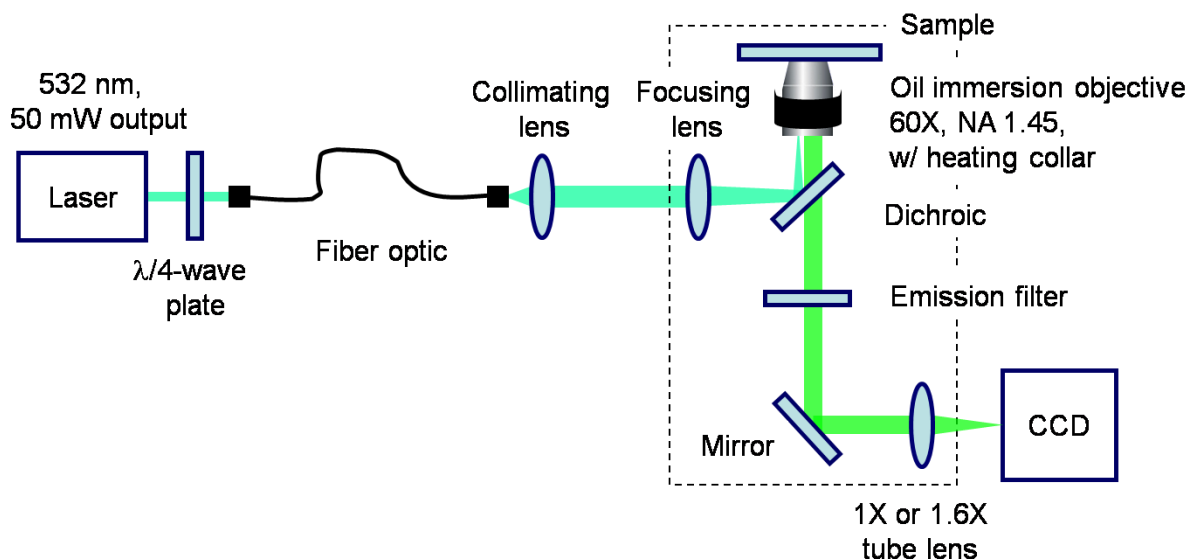
Figure S10: Schematic of the objective-based total internal reflection microscope (TIRFM). Optics within the microscope body are shown inside the dashed rectangle.

Data acquisition. Single fluorescent DiIC$_{18}$ molecules in pNIPAAm acted as the fluorescent probe and target media and each frame was acquired with a 30 ms exposure, using frame transfer so that there was no delay time between frames. Optimum laser power was determined by matching the turn-over rate, when saturation of the fluorophore is reached and S/N is maximized.[7] Single molecule fluorescence collection parameters - exposure time, detector pre-amp and electron multiplication gain - were optimized in order to achieve a S/N of at least 10, which is especially important in single molecule tracking experiments to achieve reasonable localization.[8] The acquisition protocol produced videos consisting of 1000 frames, which were obtained at 25°C with water as the solvent.

16

Single molecule diffusion simulations. Simulations were carried out in a modified Matlab program based on code originally developed by Coscoy *et al.*[2] The program generates *n_walks* random walks (number of particles) of *n_steps* steps (length of trajectories) on a Cartesian coordinate system. A Gaussian distribution of step sizes is simulated with mean 0 and variance 0.8, as well as an equal number of random angles. Steps in *x*- and *y*-directions for each trajectory are determined from the step size and angle arrays from which positions are calculated based on the user-defined diffusion process and parameters. Noise on a Gaussian distribution with the assigned relative amplitude is added after steps are determined. Diffusion coefficients are assigned by the user, along with exposure time and magnification. The diffusion process can be modified to include noise, convection, zones of confinement, or intermittent regions (phases of slow and fast diffusion).

Tracking method. Single molecule tracking was carried out by first identifying a single fluorescent spot on a given frame. The spatial intensity of the spot was fit to a 2D-Gaussian profile, and the center (x_0, y_0) of the fit used to track the trajectory on succeeding frames. The experimental localization uncertainty was determined by imaging a sample of dry (immobile) Rhodamine 6G molecules on a coverslip, with the uncertainty given by the standard deviation of the obtained *x* and *y* positions, both of which were ~40 nm.

Analysis software. All methods have Matlab code available online or freely shared by the authors. Confinement level and time series analysis functions were modified to accept trajectory data from our existing tracking program and experimental setup. The statistical analysis of lateral diffusion and multistate kinetics function was modified to accept real trajectories of varying lengths since it was originally written for simulated data of constant length. Radius of

gyration code was written in Matlab by the authors. All the code needed to carry out these

analyses is available with the electronic supplemental information for this article.

Supplemental References

1   W. X. Ying, G. Huerta, S. Steinberg and M. Zuniga, *Bulletin of Mathematical Biology*, 2009, 71, 1967-2024.

2   S. Coscoy, E. Huguet and F. Amblard, *Bulletin of Mathematical Biology*, 2007, 69, 2467-2492.

3   X. J. Wang, H. L. Tu, P. V. Braun and P. W. Bohn, *Langmuir*, 2006, 22, 817-823.

4   H. Tu, C. E. Heitzman and P. V. Braun, *Langmuir*, 2004, 20, 8313-8320.

5   Z. Y. Bao, M. L. Bruening and G. L. Baker, *Journal of the American Chemical Society*, 2006, 128, 9056-9060.

6   S. Edmondson, V. L. Osborne and W. T. S. Huck, *Chemical Society Reviews*, 2004, 33, 14-22.

7   J. Schuster, F. Cichos and C. von Borczyskowski, *Optics and Spectroscopy*, 2005, 98, 712-717.

8   M. F. Paige, E. J. Bjerneld and W. E. Moerner, *Single Molecules*, 2001, 2, 191-201.